Wetting Dynamics of the Edge of a Spreading Drop

Jing-Den Chen[(a)] and N. Wada[(b)]
Schlumberger-Doll Research, Old Quarry Road, Ridgefield, Connecticut 06877-4108
(Received 10 June 1988)

We report the first explicit measurement on the profile of a spreading edge of nonvolatile liquid, in support of the theory of Hervet and de Gennes on a one-dimensional thin spreading edge. From the laser light interference patterns, the meniscus shape of the edge was reconstructed and the advancing dynamic contact angle was measured. The meniscus shape and the contact angle are in good agreement with their theory. The meniscus shape obtained at several different capillary numbers can be collapsed into one dimensionless curve, using their scaling laws.

PACS numbers: 68.45.Gd, 47.15.Gf, 68.10.Cr, 68.10.Gw

Wettability plays an important role in processes involving immiscible fluid-fluid displacement over solid surfaces. For instance, different pore-level mechanisms and results were observed for fluids with different wettability when the immiscible displacement took place in the same porous medium.[1,2] One way of characterizing the wettability of a fluid-fluid-solid system is to measure the contact angle. One of the most popular methods for measuring the contact angle is the sessile drop method, which involves depositing a liquid drop on a smooth solid surface and measuring the angle between the solid surface and the tangent to the drop profile at the drop edge. If the drop stops spreading some time after deposition, the final angle can be easily measured through a contact angle goniometer. This angle is called the advancing static contact angle θ_s. During the spreading, the angle measured is called the advancing dynamic contact angle θ. It has been found experimentally that when the drop is spreading the contact angle is greater than θ_s and the drop keeps spreading until the angle decreases to θ_s.

In a previous paper[3] one of us reported experiments on the macroscopic aspects of the dynamics of a nonvolatile liquid drop spreading on a smooth horizontal surface. The drop diameter, apex height, and dynamic contact angle were obtained from time-sequence photographs of the silhouette of the drop. These parameters were found to obey power laws in time, and the correlation equation of dynamic contact angle and capillary number was obtained. The experiments were run under such conditions that the effects of inertia and gravity are negligible, the drop is thin and nonvolatile, and the solid plane is flat and smooth. Three typical photographs can be found in Ref. 3. Because of the limit of resolution, the angle measured in this way is apparent and its dependence on the distance cannot be studied. In this paper we focus on the edge of a spreading drop using a laser light interference technique and study the meniscus shape as a function of distance and spreading speed. We also compare the experimental results with the theory of Hervet and de Gennes.[4,5] To our knowledge, this paper presents the first explicit measurement on the profile of a spreading edge, in support of their theory.

Hervet and de Gennes[4,5] extended Tanner's[6] hydrodynamic model for the motion of a spreading edge to include the effects of London–van der Waals forces. Assuming the meniscus moves with a constant profile shape, the motion of a slowly spreading thin liquid film can be described as

$$\frac{3\mu U}{h^2}=-\frac{d}{dx}\left[\sigma\frac{d^2h}{dx^2}+\frac{A}{6\pi h^3}\right], \tag{1}$$

where h is the film thickness, x is the horizontal coordinate, U is the spreading speed at the edge, σ is the liquid surface tension, μ is the liquid viscosity, and A is the Hamaker constant. The first term in the bracket of Eq. (1) describes the effects of surface tension; the second term describes the effects of van der Waals forces, which are significant when the film thickness is less than about 1000 Å. Equation (1) reduces to a dimensionless form

$$H^{-2}dH/dX-H^2d^3H/dX^3=1, \tag{2}$$

where

$$X=x/x_0, \tag{3}$$

$$H=h/h_0, \tag{4}$$

$$x_0=3^{-1/6}aC^{-2/3}, \tag{5}$$

and

$$h_0=3^{1/6}aC^{-1/3}. \tag{6}$$

Here $a\equiv(A/6\pi\sigma)^{1/2}$ and the capillary number $C\equiv\mu U/\sigma$. At large X the van der Waals–forces term is very small compared to the capillary-forces term in Eq. (1). The numerical solution, which has zero curvature for large X, to Eq. (2) is

$$H(X)\rightarrow X[3\ln(0.4X)]^{1/3},\quad \text{for } X\gg 1. \tag{7}$$

Written in dimensional form, Eq. (7) becomes

$$h(x)\rightarrow x\left[9C\ln\left(\frac{0.4x}{x_0}\right)\right]^{1/3},\quad \text{for } \frac{x}{x_0}\gg 1. \tag{8}$$

The solid sample used was a soda-lime glass plate,

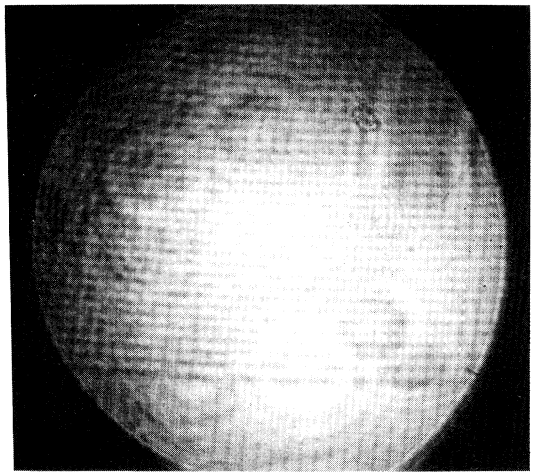

FIG. 1. Interference fringes of the edge of a spreading drop.

which was of the same material as that used in Ref. 3. The size of the soda-lime glass was $10.0\times3.5\times0.575$ cm^3. This sample was cut from a 10×10-cm^2 plate, which had a flatness of 5 μm across and a roughness of less than 0.04 μm. The cleaning procedure for the glass sample was the same as described in Ref. 3. Before each experiment the glass sample was cleaned with 2% aqueous solution of RBS-phosphote-3 concentrate (Pierce Chemical Co., Rockford, IL), rinsed with distilled water, immersed in chromic acid over night, rinsed with distilled water and acetone, and finally with distilled water. The glass sample was then dried with compressed air and laid on the leveled stage of a microscope.

The experiment involved depositing a liquid drop of approximately 0.5 μl on the cleaned glass surface and recording the interference patterns of the drop edge. The drop edge was illuminated by a parallel Ar^{++} laser beam (wavelength $\lambda=4579$ Å) through a microscope objective lens. The light-path-length correction due to the meniscus was negligible in our experiments, since θ was less than 8°. The interference patterns were recorded on a video tape by a video camera mounted on top of the microscope.

The liquids used were silicone liquids (Dow Corning 200 fluid, a dimethyl siloxane polymer, Dow Corning Corp., Midland, MI). Spreading experiments were repeated on three liquid drops. The liquid used for the first drop (drop 1) was the same as used in Ref. 3. It had a viscosity $\mu=1.96$ P, density $\rho=0.970$ g/cm^3, and surface tension against air $\sigma=20.9$ dyn/cm. The second and third drops (drops 2 and 3) had a viscosity of 9.72 P, density of 0.971 g/cm^3, and surface tension against air of 21.2 dyn/cm. Both liquids had a refractive index of $n=1.40$. According to the supplier's product information department, the number-average molecular weights of these two liquids are 7500 and 16500, respectively. The value of contact angle θ determined from the distance between the two outmost fringes at large times is as follows: 0.33° for drop 1 at 19 h after deposition, 0.37° for drop 2 at 3 d after deposition, and 0.59° for drop 3 at 1 d after deposition. All experiments were run at room temperature, 23 °C.

From the replay of the video tape, the speed of spreading U at selected points of time was determined by measuring the distance traveled by the outmost destructive interference fringe in a certain time interval around the selected time. Since the spreading was slow, we found that in our experiment U remained constant for a short period of time. The measurement error of U was less than 4% of the average of two measurements. The meniscus shape at the selected time was determined by digitizing on a video copy of the coordinates of intersection points of the interference fringes with a straight line drawn perpendicular to them. The error of reading each coordinate was less than 0.1 μm. The film thickness at the outmost destructive interference fringe is $\lambda/4n=818$ Å, and the difference in thickness between neighboring fringes is $\lambda/2n$. A typical interference pattern is shown in Fig. 1.

Since we could not measure the exact position of the three-phase contact line, we assigned the x coordinate of the outmost destructive fringe to be $x=0$ in our original digitized data of the meniscus. In order to compare with Eq. (8) we have shifted all the data points to their right by the same distance, which was determined by minimizing ms^2, the sum of the squares of difference in thickness between the experiment and Eq. (8). Here s is defined as

$$s\equiv\left[\frac{1}{m}\sum(h_e-h_t)^2\right]^{1/2},$$

where m is the number of data points, h_e is the shifted experimental thickness, and h_t is the theoretical thickness given by Eq. (8). The minimization was repeated for three different values of A: 10^{-14}, 10^{-13}, and 10^{-12} erg (Ref. 7). We found that $A=10^{-13}$ erg gave the best result for all three runs. For drop 1 the average values of s are 0.152, 0.039, and 0.098 μm, respectively, for these three values of A. For drop 1 the key parameters and comparisons with theory with $A=10^{-13}$ erg are shown in Table I and in Figs. 2, 3(a), and 4. The time in the table corresponds to the time after drop deposition. We also found that the shift distance, d, at each time increases with increasing A.

Figure 2 shows the comparison of the measured meniscus shapes of drop 1 at several different times (or different C) with Eq. (8). The experimental data are represented by symbols and the theoretical predictions by solid curves. As shown in the figure the edge of the drop becomes flatter as time increases (or C decreases). At large x the meniscus shape is almost linear. As x decreases it deviates from the straight line drawn at large x and is concave toward the air phase. This is due to the

TABLE I. Data of key parameters for Figs. 2, 3(a), and 4 for drop 1. The values of the last four parameters were calculated with $A=10^{-13}$ erg.

Time (min)	10^6C	x_0 (μm)	10^2h_0 (μm)	d (μm)	10^2s (μm)
2	6.08	0.398	1.048	4.52	7.4
6	3.96	0.530	1.209	3.11	1.5
12	2.70	0.684	1.374	3.42	1.2
20	1.93	0.856	1.537	2.41	3.2
32	1.38	1.070	1.719	2.75	2.9
35	1.32	1.102	1.744	2.76	7.7
49	0.942	1.381	1.952	3.46	4.9
70	0.594	1.877	2.276	5.29	2.3

fact that there is more viscous dissipation at smaller x. Also because of stronger viscous dissipation, the degree of concavity is more pronounced for larger C (or earlier time).

If we rescale the meniscus shape according to Eqs. (3)–(6) to a dimensionless form, we can transform Fig. 2 into Fig. 3(a). It is clear from Fig. 3(a) that all the data points in Fig. 2 at different times collapse into one curve and agree very well with the theoretical curve predicted by Eq. (7).

To compare the measured contact angle at different x with the theory, we need to differentiate the experimental data given in Fig. 2. To reduce the error in differentiation, we used a method discussed by Lanczos.[8] The method involves differentiating the second-order polynomial obtained from a least-squares fit to a set of five consecutive data points. Figure 4 shows the comparison of the contact angle between experiment and theory. Each curve in the figure corresponds to each meniscus shape shown in Fig. 2. In each curve the contact angle decreases as film thickness decreases (or x decreases). For the same x the contact angle decreases as time increases (or C decreases). As a result of differentiation most of the experimental data scatter around the theoretical curves.

In order to confirm our findings above, we repeated the experiment on two other drops (drops 2 and 3) of a different viscosity. The results of both drops 2 and 3 also show good agreement with the theory. Here we only show in Fig. 3(b) for drop 2 the comparison of the dimensionless edge shapes at different times with the theoretical curve given by Eq. (7). More details on the results will be reported elsewhere. These results confirm that the experiment was reproducible and that the exper-

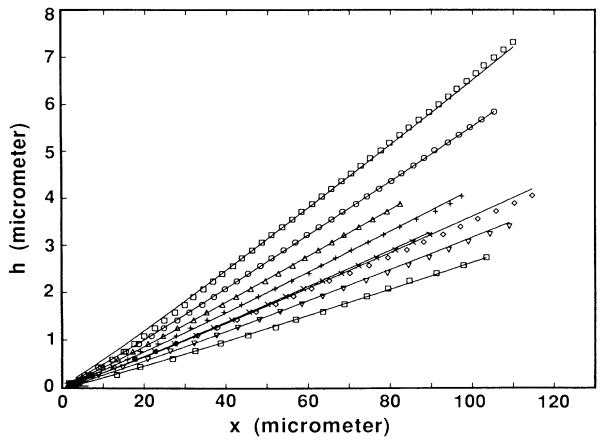

FIG. 2. Comparison of meniscus shape of the edge of drop 1 between the theory (solid curves) and the experiment (symbols) at different times: squares, 2 min; circles, 6 min; triangles, 12 min; plusses, 20 min, crosses, 32 min; diamonds, 35 min; inverted triangles, 49 min; and squares; 70 min. For some key parameters see Table I.

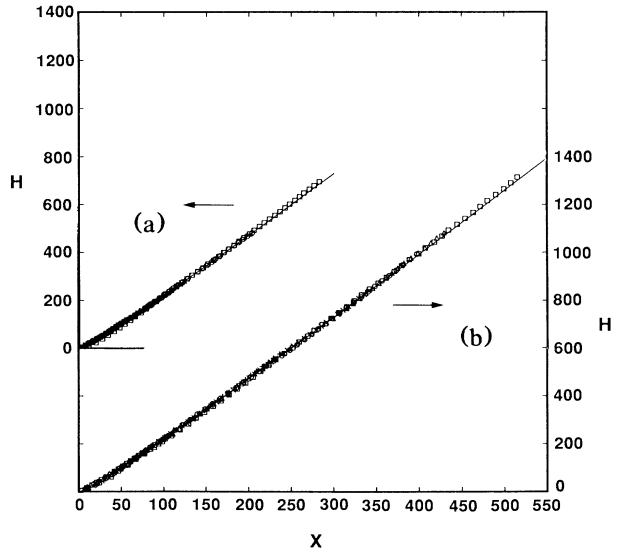

FIG. 3. Comparison of dimensionless meniscus shape between the theory (solid curve) and the experiment (symbols) at different times for (a) drop 1 and (b) drop 2. Note that all data points in Fig. 2 collapse into one curve as shown in (a).

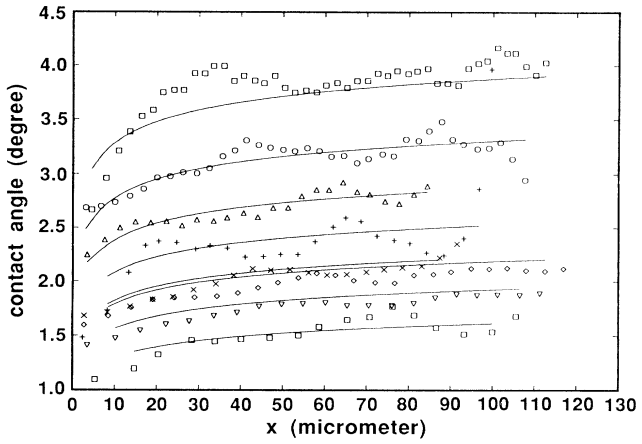

FIG. 4. Comparison of the contact angle as a function of horizontal coordinate between the theory (solid curve) and the experiment (symbols) for drop 1 at different times. Symbols have the same meaning as in Fig. 2.

iments on drops of two different viscosities agree with the theory. We should point out that the wetting phenomenon is very sensitive to the cleanliness of the system and the roughness and flatness of the solid surface. In the experiment the edge spread over a certain area on the glass surface. If the solid surface was not clean, flat or smooth enough, or the drop surface had nonuniform surface tension caused by a contaminant or a volatile component, the data obtained at a different time or for a different drop would not be consistent with each other and agree with theory. The reproducibility of the experiment and the agreement with the theory indicate that our cleaning procedure, experimental methods, and solid and liquid samples are satisfactory.

In conclusion, we have reported the first explicit measurement on the profile of a spreading nonvolatile liquid drop, in support of the theory of Hervet and de Gennes on a one-dimensional thin spreading edge. The experiments were run under the following conditions: The nonvolatile drop was spreading on a smooth horizontal plane with negligible effects of gravity and inertia. The assumptions in their theory are satisfied by these and other conditions: slow spreading speed, small slope of the edge, small length scale of the drop edge compared to the drop diameter, and large film thickness compared to the effective range of van der Waals forces. The value of C is less than about 3.7×10^{-5}; the contact angle is less than 8°, and the region of interest has a length of about 100 μm compared to the drop diameter of at least 3 mm. Except for the first outmost fringe, the thickness at other fringes is at least 2453 Å, which is large enough that the effects of van der Waals forces are negligible.

[a]Current address: Mead Imaging, 3385 Newmark Drive, Miamisburg, OH 45342.

[b]Current address: Department of Physics, Colorado School of Mines, Golden, CO 80401.

[1]J. D. Chen and J. Koplik, J. Colloid Interface Sci. **108**, 304 (1985).

[2]J. D. Chen, J. Colloid Interface Sci. **110**, 488 (1986).

[3]J. D. Chen, J. Colloid Interface Sci. **122**, 60 (1988).

[4]H. Hervet and P. G. de Gennes, C R Acad. Sci. **299II**, 499 (1984).

[5]P. G. de Gennes, Rev. Mod. Phys. **57**, 827 (1985).

[6]L. H. Tanner, J. Phys. D **12**, 1473 (1979).

[7]J. Visser, Adv. Colloid Interface Sci. **3**, 331 (1972). This review shows that for most systems the values of A usually range from 10^{-14} to 10^{-12} erg.

[8]C. Lanczos, *Applied Physics* (Prentice Hall, Englewood Cliffs, NJ, 1956), pp. 321–323.

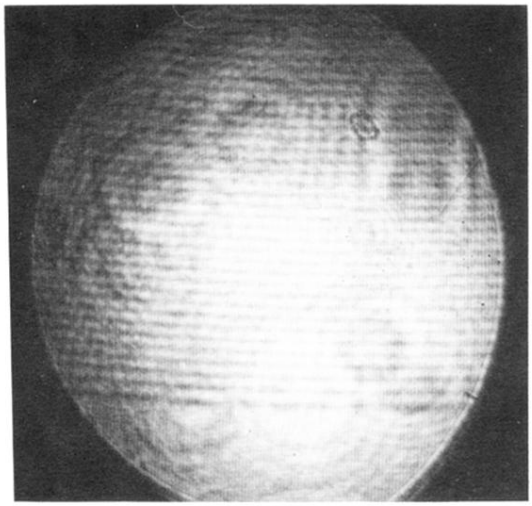

FIG. 1. Interference fringes of the edge of a spreading drop.